

## HOLOGRAPHY WITH SPATIALLY NONCOHERENT LIGHT

(x-ray diffraction microscopy; image synthesis;  
"3-dimensional photography"; T/E)

George W. Stroke and Robert C. Restrick III

The University of Michigan  
Ann Arbor, Michigan  
(Received September 1965)

Fourier-transform holography<sup>1-5</sup> with coherent light has recently permitted very considerable mathematical and experimental simplicity to be introduced into the field of "wavefront-reconstruction imaging," originated by D. Gabor in 1948. Spatial coherence in the objects (i.e. the capability of the various object points to interfere with each other, or with a "reference" field) has generally appeared to be essential to the recording of holograms. One possibility of an exception to this assumption was indicated by Stroke and Funkhouser,<sup>6</sup> and is related to their method in which a spectroscopic Fourier-transform hologram is recorded with *spectrally* noncoherent light, in a two-beam Michelson Twyman-Green interferometer, and used to produce spectra directly (without computing) by a second Fourier transformation, in the focal plane of a lens. (Many schemes for noncoherent light holography, other than that which we describe here are conceivable. Several suggestions have been made in the literature and elsewhere,<sup>7-9</sup> and the general desirability of achieving holography in noncoherent light has again been recently stressed by E. N. Leith,<sup>10</sup> but no results appear to have been reported).

In this Letter we show theoretically, and demonstrate experimentally, that image-forming Fourier-transform holograms can indeed be recorded with extended, *spatially noncoherent* monochromatic objects, and that high-quality images can be reconstructed from them, by a second Fourier transformation (e.g. in the focal plane of a lens).

The essence of our method consists in producing, in the hologram, one sinusoidal interference-grating per object point, with the correct spatial frequency and orientation, in such a way that the various gratings are made to add in *intensity*, thus recording the spatial Fourier-transform of the intensity distribution in the object. The desired intensity summation in the hologram is made possible precisely because of the noncoherence of the various object points with each other. Paradoxically, therefore, noncoherence between the various object points is a requirement for holography in noncoherent light.

As a model, we discuss a beam-splitting arrangement, in which the projection of the object onto a

plane (vector-coordinate  $\vec{\xi}$ ) produces two equally intense images  $I(\vec{\xi})$  and  $I(-\vec{\xi})$ , related to each other by a two-fold rotation<sup>5</sup> about a  $z$  axis normal to the plane  $\vec{\xi}$  (see f.ex. Fig. 1). Because of the spatial noncoherence of the various object points  $I(\vec{\xi}_1)$ ,  $I(\vec{\xi}_2)$ , . . .  $I(\vec{\xi}_n)$ , each object point interferes only

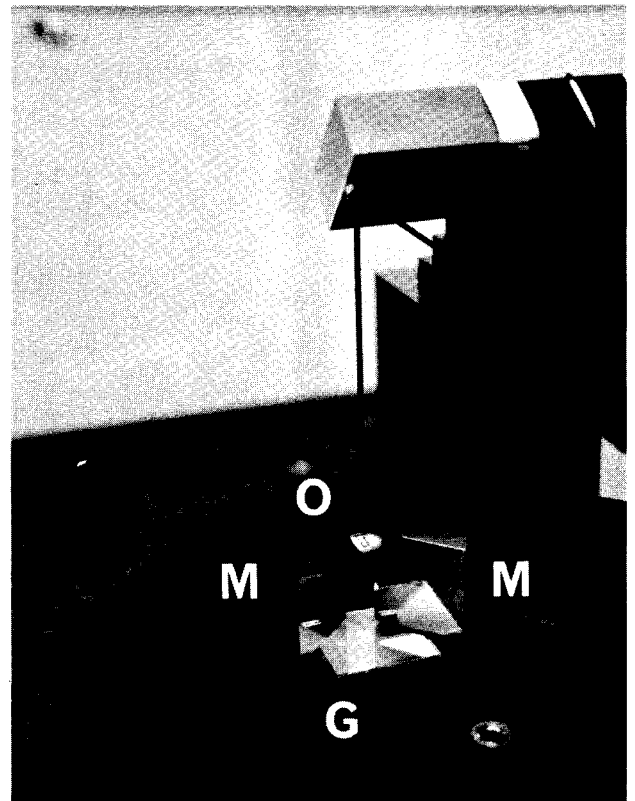


Fig. 1. Beam-splitting arrangement used for the recording of "lensless" Fourier-transform hologram in *noncoherent* light (see text), as seen from the hologram plane region. The object  $O$  (equal to the letter "R") is illuminated from above (indicated by vertical black line) and is made to produce two images by the mirrors  $M, M$ , upon "beam-splitting" diffraction by the grating  $G$ . Note the two-fold rotation with respect to each other of the two images, seen on the mirrors  $M, M$ . (The image "R" appearing on the grating surface, directly below the object, is due to surface scattering, and is not seen by the hologram.) The grating-dimensions ( $55 \times 55$  mm) give the scale of the arrangement. The Fourier-transform hologram was recorded on a Kodak 649F plate, at a distance  $f = 1$  m from  $M, M$ , without the intervention of any additional optical elements.

with its respective "mirror" image  $I(-\bar{\xi}_1)$ ,  $I(-\bar{\xi}_2)$ , . . .  $I(-\bar{\xi}_n)$ , to produce, on a hologram plane  $\bar{x}_2$  normal to the  $z$  axis at a distance  $z = f$  from the  $\bar{\xi}$  plane, a fringe system of a frequency and orientation characteristic of that object point only. The resultant intensity  $I(\bar{x})$  recorded on the hologram is given by the equation

$$I(\bar{x}) = \int I(\bar{\xi}) \left[ 1 + \cos 2\pi \frac{\bar{x}}{\lambda} \bullet \frac{2\bar{\xi}}{f} \right] d\bar{\xi}$$

(where  $\bullet$  indicates a vector dot product, and  $\lambda$  is the wavelength). The hologram intensity  $I(\bar{x})$  given by Eq. (1) is recognized as formed of a constant ("dc") term, plus the cosine Fourier transform of the intensity distribution  $I(\bar{\xi})$  in the object.<sup>6</sup> Consequently, illumination of the hologram with a spatially coherent, monochromatic plane wave will produce, by Fourier transformation in the focal plane of a lens, two images  $I(\bar{\xi})$ , symmetrically displayed on the two sides of the optical axis (together with a "dc" image, centered on the axis).

The beam-splitting arrangement used in our experiments is shown in Fig. 1, together with the object (letter "R") illuminated with spatially noncoherent light. A reconstruction of the image of the letter "R" is shown in Fig. 2. The actual beam splitter used in this case was an optical diffraction grating,<sup>11</sup> with a spacing of 1180 grooves/mm, and having a groove form shaped to produce two equally intense first orders, without polarization.<sup>11,12</sup> The spatial noncoherence with the monochromatic 6328 Å laser light used was achieved by imaging a rapidly moving diffuser onto the object plane. (The success in having indeed achieved the desired noncoherence with the moving diffuser and the laser used, was verified by also recording a hologram with the diffuser maintained stationary, so as to maintain spatially coherent light:<sup>13</sup> the reconstruction, in this case, can be readily shown<sup>5</sup> to consist of a convolution of  $I(\bar{\xi})$  with itself, rather than of images of  $I(\bar{\xi})$ ). A reconstruction of the "images" from the

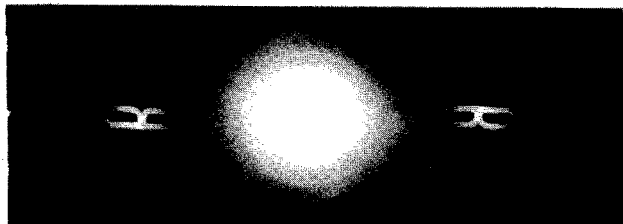


Fig. 2. Fourier-transform reconstruction of the images of the letter "R," from the hologram recorded in *spatially noncoherent light* in the arrangement of Fig. 1.

hologram recorded with spatially coherent light, under these conditions, is shown in Fig. 3.)

We wish to note the possible applicability of our method of "lensless" Fourier-transform holography with noncoherent light to image-forming x-ray microscopy, especially because of the possible use of grating-like and beam-splitting properties of crystals. We have previously stressed<sup>2-5</sup> the high-resolution advantages of Fourier-transform holograms compared to Fresnel-transform holograms. The "plane-wave" summation property (or its spherical-wave equivalent)<sup>3</sup> inherent in Fourier-transform holography, and its related absence of aberrations, is clear, also in analogy with similar advantages of plane vs concave gratings.<sup>11</sup>

We wish to acknowledge the generous support of a part of this work by the National Science Foundation and the kindness of the Jarrell-Ash Company in providing the beam-splitting grating.

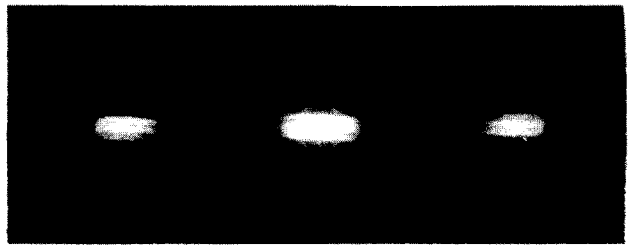


Fig. 3. Fourier-transform reconstruction of "images" (central "dc" term and two side-band images) from hologram recorded in *spatially coherent light* (obtained by maintaining stationary the diffuser focused onto the object in Fig. 1) to verify that spatial noncoherence was indeed obtained in the recording of the hologram for Fig. 2, by moving the diffuser during the exposure (see text).

<sup>1</sup>G. W. Stroke, *An Introduction to Optics of Coherent and Non-Coherent Electromagnetic Radiations*, 1st edition (The University of Michigan, Ann Arbor, 1964) 77 pages.

<sup>2</sup>G. W. Stroke and D. G. Falconer, *Phys. Letters* **13**, 306 (1964).

<sup>3</sup>G. W. Stroke, *Appl. Phys. Letters* **6**, 201 (1965).

<sup>4</sup>D. Gabor, G. W. Stroke, R. Restrick, A. Funkhouser, and D. Brumm, *Phys. Letters* **18**, 116 (1965).

<sup>5</sup>G. W. Stroke, R. Restrick, A. Funkhouser, and D. Brumm, *Phys. Letters* **18**, 274 (1965).

<sup>6</sup>G. W. Stroke and A. Funkhouser, *Phys. Letters* **16**, 272 (1965).

<sup>7</sup>L. Mertz, *J. Opt. Soc. Am.* **54**, No. 10, p. IV (1965).

<sup>8</sup>J. T. Winthrop and C. R. Worthington, *Phys. Letters* **15**, 124 (1965).

<sup>9</sup>G. Cochran, *J. Opt. Soc. Am.* **55**, 615 (1965).

<sup>10</sup>E. N. Leith and J. Upatnieks, *Physics Today* **18**, No. 8 (1965) p. 26.

<sup>11</sup>G. W. Stroke, "Diffraction Gratings" in *Handbuch der Physik*, Vol. 29, ed. S. Flügge (Springer Verlag, Berlin and Heidelberg, 1965) in print.

<sup>12</sup>G. W. Stroke, *Phys. Letters* **5**, 45 (1963).

<sup>13</sup>G. W. Stroke and D. G. Falconer, *Phys. Letters* **15**, 238 (1965).

<sup>14</sup>G. W. Stroke, "Attainment of High Resolutions in Image-Forming X-ray Microscopy with 'Lensless' Fourier-Transform

Holograms and Correlative Source-Effect Compensation," in *Proceedings of the IVth X-Ray Congress* (Paris, 7-10 September 1965) (Hermann, Paris) in print.

## FLUX CREEP AS A DOMINANT SOURCE OF DEGRADATION IN SUPERCONDUCTING SOLENOIDS

(Nb-25% Zr; thermal instability; E)

Y. Iwasa and D. Bruce Montgomery

National Magnet Laboratory<sup>1</sup>

Massachusetts Institute of Technology

Cambridge, Massachusetts

(Received 9 September 1965)

In this Letter we report experimental evidence that the mechanism of unstable flux creep arising from thermal instabilities as suggested by Anderson<sup>2</sup> and by Anderson and Kim<sup>3</sup> is responsible for the current degradation commonly observed in superconducting solenoids.

Transient flux creep was induced in a sample by means of suitable magnetic field pulses. With the sample carrying a transport current, the resistivity arising during flux creep produced transient joule heating, and when the current was large enough, the heating was sufficient to exceed the local critical temperature, thereby resulting in a quench.

Field pulses of varying amplitudes and rise times were applied to a noninductively wound specimen consisting of about 50 ft of 0.010-in. diam insulated Nb-25% Zr commercial wire. The wire had no copper cladding. Our apparatus was designed to allow sample transport currents up to 60 A, to provide an ambient background field up to 40 kG, and to monitor continuously the magnetization of the sample. To ensure that the entire sample was in the critical state as defined by Kim et al.,<sup>4</sup> the transport current was introduced first and then the ambient field was swept until the sample followed the critical-state curve. When the desired field was reached the sweep was stopped and a field pulse was applied in a direction which enhanced the ambient field. If the sample did not quench, the cycle was repeated with increasing values of transport current until a quench was obtained.

Typical data are shown in Fig. 1 for 125- $\mu$ sec and 20- $\mu$ sec rise time pulses. The data exhibit four distinct features: (1) there is a threshold in the amplitude of a pulse below which no degradation occurs; (2) the threshold pulse amplitude for degradation decreases as the pulse rise time,  $dHp/dt$ , is increased; (3) for a given rise time, there is no further decrease

in the degraded current for pulses greater than a certain amplitude; and (4) there is an area of maximum sensitivity to pulses centered about 15 kG.

The data in Fig. 1, together with data taken at 50- $\mu$ sec and 270- $\mu$ sec rise times are presented in a different manner in Fig. 2. The abscissa is the product of the peak value of the pulse  $H_{p0}$  and the maximum rising rate of pulse field with respect to time,  $dHp/dt$ . The ordinate is the ratio of threshold quenching current to the published short sample data. Since the term  $H_{p0}(dHp/dt)$  is proportional to  $dHp^2/dt$ , it is proportional to the real power input during the pulse rise. We interpret the very sharp vertical transition in Fig. 2 as specifying the local power dissipation necessary to produce a thermal instability and unstable creep. The lowest transition in Fig. 2 approaches  $H_{p0}(dHp/dt) = 10$  G-G/ $\mu$ sec just below 13.5 kG. This means, for example, that a pulse with about 1- $\mu$ sec rise time would need an amplitude less than  $\sqrt{10}$  G to precipitate unstable flux creep. These very small required values of trigger pulses reflect the extreme sensitivity of flux creep to become unstable under minute thermal perturbations ( $10^{-3} < \Delta T/T < 10^{-2}$ ) as predicted by Anderson and Kim.<sup>3</sup>

The threshold value of transport current to which the short sample current degrades is interpreted as that current which causes sufficient joule heating at the value of creep resistivity to quench the sample. The magnetic field pulse serves only to initiate unstable creep. Once established, the resultant resistivity is independent of  $H_{p0}(dHp/dt)$  and considerable increases in pulse power beyond the threshold value result in no further degradation. The threshold current should not be confused with the so-called "minimum propagating current" which is the current that will cause a normal front to propagate once a local region has been driven normal. The